The Aeronautical Journal (2024), **128**, pp. 73–91
doi:10.1017/aer.2023.38

REGULAR PAPER

Cooperative trajectory shaping guidance law for multiple anti-ship missiles

G. Yang[1], Y. Fang[2], W. Ma[3], S. Zhu[4] and W. Fu[2]

[1]School of Marine Science and Technology, Northwestern Polytechnical University, Xi'an, China, [2]Unmanned System Research Institute, Northwestern Polytechnical University, Xi'an, China, [3]School of Automation, Northwestern Polytechnical University, Xi'an, China and [4]School of Astronautics, Northwestern Polytechnical University, Xi'an, China
Corresponding author: W. Fu; Email: wenxingfu@nwpu.edu.cn

Received: 4 January 2023; **Revised:** 7 April 2023; **Accepted:** 12 April 2023

Keywords: Shaping cooperative guidance law; Optimal energy management; Finite-time convergence

Abstract
To enhance the performance of anti-ship missiles cooperative attack, this paper proposes a finite-time trajectory shaping-based cooperative guidance law (TSCGL). Firstly, the cooperative guidance model is established on segmented linearisation of the missile's heading angle. Then, a trajectory shaping guidance law for a single missile is derived by a weighted optimal energy cost function and Schwarz inequality. On this basis, a finite-time TSCGL is proposed combined with trajectory shaping technology and finite-time theory. The desirable finite-time convergence performance can ensure a simultaneous attack. Through an improved method of time-to-go estimation, it is independent of small-angle assumption and relaxes the launching conditions of the missiles. Additionally, the proposed finite-time TSCGL can achieve better damage performance through energy management. Finally, simulation results demonstrate the effectiveness and superiority of the proposed finite-time TSCGL.

Nomenclature

a_i	guidance command of the i-th missile (m/s^2)
a_{ci}	cooperative term of the a_i (m/s^2)
a_{si}	basis shaping guidance term of the a_i (m/s^2)
A	system matrix
A_G	adjacency matrix of graph G
B	control matrix
E	edge set of graph
G	communication network graph
J	cost function $((m/s^2)^2)$
k	design parameter of the sliding surface
L	Laplace matrix of the graph G
M_i	i-th missile
q_i	line-of-sight (LOS) angle of the i-th missile (deg)
r_i	relative distance of the i-th missile (m)
s_i	sliding surface of the i-th missile (s)
t_{goi}	time-to-go of the i-th missile (s)
t_{0i}	initial impact time of the i-th missile (s)
t_{fi}	final impact time of the i-th missile (s)
T	target
u	guidance command (m/s^2)
u^*	optimal guidance command (m/s^2)
u_i^{nom}	the consensus protocol
v_{yi}	vertical component of V_{mi} (m/s^2)

v_{y0i}	initial vertical component of V_{mi} (m/s^2)
v_{yfi}	final vertical component of V_{mi} (m/s^2)
V	set of vertices
V_{mi}	speed of the i-th missile (m/s)
V_{1i}, V_{2i}	different Lyapunov functions of the i-th missile
W	weight function
X	state of i-th missile
X_T, Y_T	current position of the target
X_{TP}, Y_{TP}	predicted interception point of the target
y_i	altitude of the i-th missile (m)

Greek Symbol

β_i	design parameter of the i-th missile's consistency protocol
η_i	lead angle of the i-th missile (deg)
γ_i	heading angle of the i-th missile (deg)
γ_{0i}	segmented linearisation point of the i-th missile's heading angle (deg)
$\Delta\gamma_i$	a small value, equals to $\gamma_i - \gamma_{0i}$ (deg)
γ_{di}	desired heading angle of the i-th missile (deg)
γ_{fi}	final heading angle of the i-th missile (deg)
Φ	state transition matrix
θ_T	heading angle of target
ε	design parameter of the sliding surface

1.0 Introduction

Shaping guidance law as an efficient guidance scheme has been widely used in the research of naval attack and defense [1–4]. The shaping guidance law can ensure a single missile attack the target with optimal energy and achieve the desired accuracy and damage performance. Even though the shaping guidance law is effective in most traditional scenarios, a single missile is difficult to penetrate for a modern warship equipped with missile defense systems [5, 6]. Therefore, cooperative guidance organised by multiple missiles can ensure that more than one missile hits the target, which greatly increases the success rate of the operation [7, 8]. Jeon, I.S. et al. [9] conducted impact time control guidance (ITCG) law, so as to anti-ship missiles can intercept a stationary target with the prescribed impact time. Inspired by this idea, a shaping cooperative guidance law to control impact time and angle was presented in Refs. [10–13].

As a core factor in shaping cooperative guidance law, the estimation of the time-to-go can significantly influence guidance performance. It can be noted that the studies mentioned above are established on the small-angle assumption in estimation [10, 11], which limits the generalisation of the investigations. Therefore, various methods are proposed to improve the accuracy of the estimation in Refs. [14–16]. Liu, S. et al. [16] proposed an improved estimation method of time-to-go, in which the calculation accuracy can be guaranteed with a large initial lead angle. Although enough efforts have been devoted to the accuracy improvement of estimation, without energy management, constraints of energy will limit the execution or even lead to the failure of cooperation. In view of the difficulty in energy management, the optimal shaping cooperative guidance has been widely discussed in Refs. [17–20]. Chen, X. et al. [17] derived an optimal guidance law wherein cooperative impact time and angle constraints can be satisfied. Adding a compensation term to the guidance law, Liu J. et al. [18] derived a multi-missile optimal cooperative guidance law by optimal control theory.

To ensure penetration capability, guidance laws based on consensus theory have been established for cooperation. Multiple anti-ship missiles can perform a saturation attack on the target by exchanging information. Hence, consensus-based cooperative guidance laws have been widely studied to ensure the impact time. However, the asymptotic convergence is insufficient for a transient flight. As an extension, the finite-time shaping cooperative guidance law has become a hotspot in engineering practice [21–23]. Sinha, A. et al. [24] proposed a leader-follower cooperative salvo guidance strategy to intercept

https://doi.org/10.1017/aer.2023.38 Published online by Cambridge University Press

stationary targets by exploiting the advantages of supertwisting sliding mode control. Based on powered missiles, some cooperative guidance laws aim to control the axial speed in the direction of LOS to fulfill the cooperation of impact time [22, 25, 26]. Liu, S. et al. [27] designed a finite-time convergence cooperative guidance law from two directions of the LOS, which can easily satisfy the impact time and angle constraint. Although the powered missiles hold better adjustment capability, their cost increases the economic burden for cooperation. Therefore, it is more practical to study the cooperative guidance law for unpowered missiles without speed control [28, 29]. Shin, H.S. et al. [30] designed a finite-time guidance law to nullify the LOS angular rate to address the terminal guidance problem of missiles intercepting targets in three-dimensional space. With the measured initial conditions, the boundary of convergence time can be adjusted by turning parameters. Without energy engagement, however, the execution of guidance command is limited. Hence, fast convergence with optimal energy management is still a challenge for application.

The aforementioned guidance laws have made great progress, but the problem of optimal shaping cooperative guidance law design remains open. (1) The estimation of the time-to-go with the small angle assumption hinders the engineering application of the cooperative guidance law. (2) Optimal energy control needs to be considered to ensure cooperative performance. (3) Fast convergence speed for state variables is necessary in the guidance process.

Inspired by the above discussions, a finite-time trajectory shaping-based cooperative guidance law (TSCGL) is proposed, which can achieve multiple missile cooperation with desired damage and convergence performance. The main contributions are summarised as follows:

(1) The proposed finite-time TSCGL can ensure impact time and angle constraints, so as to achieve simultaneous attack with desired damage performance. Different from most existing studies in Ref. [31], independent of small-angle assumption, the proposed finite-time TSCGL holds higher accuracy of impact time estimation, even in the case of a large initial leading angle.

(2) Compared with existing optimal shaping guidance law in Ref. [2], the proposed TSCGL can guarantee optimal energy management without simplifying terminal boundary conditions. Based on the weighted optimal energy cost function, the stability of the optimal TSCGL is derived by the Schwarz inequality.

(3) The proposed finite-time TSCGL can achieve better convergence performance. Compared with asymptotic cooperative guidance law in Ref. [32], the final impact time can converge within a finite time.

The rest of the paper is organised as follows. Section 2.0 gives problem descriptions and relative models. Section 3.0 mainly derives the optimal guidance command of the shaping guidance law and the determination of cooperative guidance law. In Section 4.0, numerical simulations for four cases are conducted to demonstrate the effectiveness and advantages of the cooperative shaping guidance law. Section 5.0 gives the conclusions of this paper.

2.0 Problem formulation and model derivation

Multiple missiles-target engagement geometry in vertical plane is shown in Fig. 1. The notations M_i and T represent the i-th missile and target. V_{mi}, a_i, r_i, y_i, q_i, η_i and γ_i denote speed, guidance command, relative distance, altitude, line of sight (LOS) angle, lead angle and heading angle of the i-th missile, $i = 1, 2, \cdots, m$.

The relative motion model of the i-th missile are given as

$$\dot{r}_i = -V_{mi}\cos(\eta_i) \tag{1}$$

$$\dot{q}_i = V_{mi}\sin(\eta_i)/r_i \tag{2}$$

$$\dot{\gamma}_i = a_i/V_{mi} \tag{3}$$

$$\eta_i = q_i - \gamma_i \tag{4}$$

https://doi.org/10.1017/aer.2023.38 Published online by Cambridge University Press

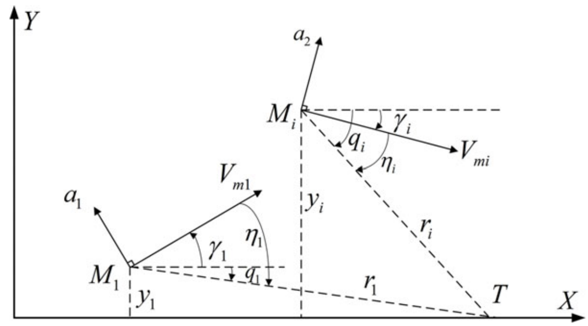

Figure 1. *Multiple missiles-target engagement geometry.*

The guidance command a_i is constructed as

$$a_i = a_{si} + a_{ci} \tag{5}$$

where a_{si} and a_{ci} are the basis shaping guidance term and cooperative term.

The core of multiple missiles cooperatively attacking the target is that they can satisfy the constraints of both time convergence and interception accuracy. In addition, in order to improve damage performance on the target, impact angle and energy consumption should be taken into consideration. Generally, the impact angle constraint translates into controlling the heading angle at interception [2, 4]. Thus, the design objective of the finite-time TSCGL can be described as follows:

$$\begin{cases} \lim\limits_{t \to t_f} (t_{goi} - t_{goj}) \to 0 \\ \lim\limits_{t \to t_f} r_i \to 0 \\ \lim\limits_{t \to t_f} \gamma_i \to \gamma_{di} \\ \lim\limits_{t \to t_f} \min J \end{cases} \tag{6}$$

where t_{go} is the time-to-go, γ_{di} denotes desired heading angle and J represents cost function.

3.0 Guidance law design

Before designing the finite-time TSCGL, some preliminary assumptions need to be put forward:

Assumption 1. *Anti-ship missiles and ship are viewed as mass points.*

Assumption 2. *Compared to missiles, the ship can be considered a stationary target.*

Assumption 3. *All the velocities of unpowered missiles are assumed to be fixed with adjustable perpendicular acceleration throughout the engagement.*

3.1 Derivation of shaping guidance law

The cost function is definited as

$$\min J = \frac{1}{2} \int_t^{t_{fi}} W(\tau) u^2(\tau) d\tau \tag{7}$$

where $W(t) > 0, t \in \left(t_{0i}, t_{fi}\right)$. t_{0i} and t_{fi} are the initial time and the final impact time of the i-th missile.

Considering that the kinematics of the i-th missile are established by

$$\dot{y}_i = V_{mi} \sin \gamma_i \tag{8}$$

https://doi.org/10.1017/aer.2023.38 Published online by Cambridge University Press

Linearisation at point γ_{0i} of segment k are as follows

$$\dot{y}_i = V_{mi}\sin(\gamma_{0i}) + V_{mi}\Delta\gamma_i\cos(\gamma_{0i}) = v_{yi} \tag{9}$$

where $\gamma_i = \gamma_{0i} + \Delta\gamma_i$. $\Delta\gamma_i$ is a small value and γ_{0i} is a constant in the k segment. v_{yi} is the vertical component of V_{mi}. Derivations are derived as

$$\ddot{y}_i = V_{mi}\dot{\Delta\gamma_i}\cos(\gamma_{0i}) = \dot{v}_{yi} \tag{10}$$

$$\dot{\gamma}_i = \dot{\Delta\gamma_i} \tag{11}$$

Then, based on Equation (3), one can be obtained as

$$\ddot{y}_i = a_i\cos(\gamma_{0i}) = \dot{v}_{yi} \tag{12}$$

The linearised kinematic Equations (9) and (10) can be rewritten in the matrix form as

$$\dot{x} = Ax + Bu \tag{13}$$

where

$$\begin{gathered} x \triangleq \begin{bmatrix} y_i & v_{yi} \end{bmatrix}^T, u \triangleq a_i \\ A \triangleq \begin{bmatrix} 0 & 1 \\ 0 & 0 \end{bmatrix}, B \triangleq \begin{bmatrix} 0 \\ cos(\gamma_{0i}) \end{bmatrix} \end{gathered} \tag{14}$$

Based on the linear control theory, the solution of Equation (13) can be expressed as

$$x(t_{fi}) = \Phi(t_{fi} - t)\, x(t) + \int_t^{t_{fi}} \Phi(t_{fi} - \tau)\, Bu(\tau)\, d\tau \tag{15}$$

$$\Phi(t_{fi} - t) = e^{A(t_{fi}-t)} \tag{16}$$

where $\Phi(t)$ is the state transition matrix of the linear system as Equation (13). Expand the right side of Equation (16) as follow

$$e^{A(t_{fi}-t)} = I + A(t_{fi} - t) + \frac{A^2}{2!}(t_{fi} - t)^2 + \cdots \tag{17}$$

Calculating the right side of Equation (15) and omitting the high order terms, we can obtain

$$x(t_{fi}) = \begin{bmatrix} 1 & t_{fi} - t \\ 0 & 1 \end{bmatrix} x(t) + \int_t^{t_{fi}} \begin{bmatrix} 1 & t_{fi} - t \\ 0 & 1 \end{bmatrix} \begin{bmatrix} 0 \\ cos(\gamma_{0i}) \end{bmatrix} u(\tau)\, d\tau \tag{18}$$

Using shorthand notations as

$$\begin{aligned} & f_1 \triangleq x_1(t) + (t_{fi} - t)\, x_2(t) - x_1(t_{fi}), h_1(\tau) \triangleq -cos(\gamma_{0i})\,(t_{fi} - t) \\ & f_2 \triangleq x_2(t) - x_2(t_{fi}), \qquad\qquad h_2(\tau) \triangleq -\cos(\gamma_{0i}) \end{aligned} \tag{19}$$

Equation (15) can be rewritten as

$$\begin{cases} f_1 = \int_t^{t_{fi}} h_1(\tau)u(\tau)d\tau \\ f_2 = \int_t^{t_{fi}} h_2(\tau)u(\tau)d\tau \end{cases} \tag{20}$$

By introducing a new variable denoted as λ, then by Equation (20) we can obtain

$$f \triangleq f_1 - \lambda f_2 = \int_t^{t_{fi}} [h_1(\tau) - \lambda h_2(\tau)]\, u(\tau)d\tau \tag{21}$$

Furthermore, Equation (21) can be transformed as

$$f = \int_t^{t_{fi}} (h_1(\tau) - \lambda h_2(\tau))\, W^{1/2}(\tau)W^{-1/2}(\tau)u(\tau)\mathrm{d}\tau \tag{22}$$

https://doi.org/10.1017/aer.2023.38 Published online by Cambridge University Press

Based on the Schwarz inequality, the following inequality can be obtained as

$$\frac{f^2}{2\int_t^{t_{fi}}[h_1(\tau)-\lambda h_2(\tau)]^2 W^{-1}(\tau)\mathrm{d}\tau} \leq \frac{1}{2}\int_t^{t_{fi}} W(\tau)u^2(\tau)\mathrm{d}\tau \tag{23}$$

It is obvious that the right side of Equation (23) equals the cost function defined in Equation (12). In other words, it provides a lower bound for the minimum cost function. According to the Schwarz inequality, the condition of inequality Equation (23) becoming the equation is that the guidance command must be as

$$u(t) = K[h_1(t) - \lambda h_2(t)]\, W^{-1}(t) \tag{24}$$

where K is a constant to be determined. Substituting Equation (24) into Equation (19), the constant K can be obtained as

$$K = \frac{f_1}{\int_t^{t_{fi}} h_1^2(\tau)W^{-1}(\tau)d\tau - \lambda\int_t^{t_{fi}} h_1(\tau)h_2(\tau)W^{-1}(\tau)d\tau} \tag{25}$$

To facilitate the derivation, some notations are given as follows

$$\begin{cases} g_{1i} \triangleq \int_t^{t_{fi}} h_1^2(\tau)W^{-1}(\tau)d\tau \\ g_{2i} \triangleq \int_t^{t_{fi}} h_1(\tau)h_2(\tau)W^{-1}(\tau)d\tau \\ g_{3i} \triangleq \int_t^{t_{fi}} h_2^2(\tau)W^{-1}(\tau)d\tau \end{cases} \tag{26}$$

Thus Equation (25) can be rewritten as

$$K = \frac{f_1}{g_{1i} - \lambda g_{2i}} \tag{27}$$

Substituting Equation (27) into Equation (24), the guidance command can be obtained as

$$u(t) = \frac{f_1\,[h_1(t) - \lambda h_2(t)]\, W^{-1}(t)}{g_{1i} - \lambda g_{2i}} \tag{28}$$

From Equation (23), the minimum value of cost function can be expressed as

$$J = \frac{(f_1 - \lambda f_2)^2}{2(g_{1i} - 2\lambda g_{2i} + \lambda^2 g_{3i})} \tag{29}$$

Taking the derivative of J with respect to λ and imposing $dJ/d\lambda = 0$, the optimal solution of λ can be expressed as

$$\lambda^* = \frac{f_1 g_{2i} - f_2 g_{1i}}{f_1 g_{3i} - f_2 g_{2i}} \tag{30}$$

Substituting Equation (30) into Equation (28), the optimal guidance command can be obtained as

$$u^*(\tau) = \frac{\left[f_1 h_1(\tau)g_{3i} - g_{2i}(f_2 h_1(\tau) + f_1 h_2(\tau)) + f_2 h_2(\tau)g_{1i}\right] W^{-1}(\tau)}{g_{1i}g_{3i} - g_{2i}^2} \tag{31}$$

Substituting Equations (14) and (19) into Equation (31), the optimal trajectory shaping guidance law is expressed as

$$a_{si} = u^*(t) = k_{1i}y_i + k_{2i}v_{yi} + k_{3i} \tag{32}$$

https://doi.org/10.1017/aer.2023.38 Published online by Cambridge University Press

where the guidance gains k_{1i}, k_{2i} and k_{3i} are given as follows

$$\begin{cases} k_{1i} = \dfrac{-t_{goi}g_{3i} + g_{2i}}{g_{1i}g_{3i} - g_{2i}^2} W^{-1}(t) \\ k_{2i} = \dfrac{-t_{goi}^2 g_{3i} + 2g_{2i}t_{goi} - g_{1i}}{g_{1i}g_{3i} - g_{2i}^2} W^{-1}(t) \\ k_{3i} = \dfrac{\left(t_{goi}g_{3i} - g_{2i}\right) y_i\left(t_{fi}\right) + \left(g_{1i} - t_{goi}g_{2i}\right) v_{yi}\left(t_{fi}\right)}{g_{1i}g_{3i} - g_{2i}^2} W^{-1}(t) \end{cases} \tag{33}$$

where $t_{goi} = \left(t_{fi} - t\right)$ is the time-to-go of the i-th missile, and g_{1i}, g_{2i}, g_{3i} are defined as

$$\begin{cases} g_{1i} = \int_t^{t_{fi}} \left(t_{fi} - \tau\right)^2 W^{-1}(\tau)d\tau \\ g_{2i} = \int_t^{t_{fi}} \left(t_{fi} - \tau\right) \cos(\gamma_{0i}) W^{-1}(\tau)d\tau \\ g_{3i} = \int_t^{t_{fi}} \cos^2(\gamma_{0i}) W^{-1}(\tau)d\tau \end{cases} \tag{34}$$

From Equation (34), the analytical solution of g_{1i}, g_{2i}, g_{3i} depend on the prescribed the final impact time t_{fi} and the weighting function $W^{-1}(t)$ which is a time-varying function. In order to achieve time-cooperative guidance for multiple missiles and remove constraint of the final impact time t_{fi}, we make the assumption as follows

$$W^{-1}(\tau) = 1 \tag{35}$$

$$\gamma_{0i} \equiv 0 \tag{36}$$

After simplification, the shaping guidance command in Equation (32) can be transformed as

$$a_{si} = -6\frac{y_i}{t_{goi}^2} - 4\frac{v_{yi}}{t_{goi}} + 6\frac{y_i(t_{fi})}{t_{goi}^2} - 2\frac{v_{yi}(t_{fi})}{t_{goi}} \tag{37}$$

Note that these results are identical to the optimal control guidance law as studied in Ref. [2]. Combining Equation (4) with Equation (9), the following equation can be obtained as

$$\dot{v}_{yi} = V_{mi}\dot{\gamma}_i \cos\gamma_{0i} \tag{38}$$

The integral of Equation (38) from 0 to t_{fi} can be expressed as

$$\int_0^{t_{fi}} \dot{v}_{yi}dt = V_{mi}\cos\gamma_{0i} \int_0^{t_{fi}} \dot{\gamma}_i dt \tag{39}$$

Then, the final speed constraint $v_{yi}(t_{fi})$ can be transformed into the heading angle constraint $\gamma_i(t_{fi})$ by

$$v_{yi}(t_{fi}) = v_{y0i} + V_{mi}\left(\gamma_i(t_{fi}) - \gamma_{0i}\right)\cos\gamma_{0i} \tag{40}$$

Remark 1. $\Delta\gamma_i$ is considered as a small value in some $\gamma_{0i}(k)$ segment (at point γ_{0i} of segment k). Once the absolute value of $\Delta\gamma_i$ is bigger than 5 degrees ($|\Delta\gamma_i| > 5^\circ$), the linearised kinematics is switched in next $\gamma_{0i}(k+1)$ segment. Furthermore, their relationship is satisfied by

$$\gamma_{0i}(k+1) = \gamma_{0i}(k) + \Delta\gamma_i \tag{41}$$

where $k = 1, 2, \cdots, n$, $\Delta\gamma_i = \pm 5^\circ$.

3.2 Derivation of cooperative shaping guidance law

In this subsection, the concept of algebraic graph theory is introduced by Ref. [27]. Suppose that communication network between missiles can be expressed as $G = \{V, E\}$, where $V = \{1, 2, \cdots, n\}$ denotes the set of vertices, $E \subseteq V \times V$denotes the edge set of graph, the subscript i denotes the i-th missile, e_{ij}

https://doi.org/10.1017/aer.2023.38 Published online by Cambridge University Press

is the edge of graph G, and $e_{ij} \subseteq E$ indicates that the agents i and j can receive message from each other in an undirected graph. If there is a connection between any two missiles in the graph, then the graph G is connected. In the directed graph, $e_{ij} \subseteq E$ means the missile i can receive message from missile$j$. In addition, $A_G = (a_{ij}) \in R^{n\times n}$ is the adjacency matrix of graph G. If $e_{ij} \subseteq E$, then $a_{ij} > 0$; $a_{ij} = 0$, otherwise. It is worth noting that $a_{ij} = a_{ji}$ when the communication topology is an undirected graph. The Laplace matrix of the graph G is defined as $L = (L_{ij}) \in R^{n\times n}$, which can be expressed as

$$L_{ij} = \begin{cases} -a_{ij} & i \neq j \\ \sum_{j=1, j\neq i}^{n} a_{ij} & i = j \end{cases} \tag{42}$$

The final impact time of the i th missile can be defined as

$$t_{fi} = t_{goi} + t \tag{43}$$

Let $X_i = t_{fi}$, a multiple missiles system is described as

$$\dot{X}_i = u_i^{nom} \tag{44}$$

where u_i^{nom} is the consensus protocol which should be designed with the information of the missile itself and its neighbours.

In order to verify the finite-time stability of the system, the following Lemma is given.

Lemma 1. [33] *Suppose that there exists a continuous positive function V_t, positive real numbers α, β and $0 < \gamma < 1$, satisfying $\dot{V}_t \leq -\alpha V(t) - \beta V^{\gamma}(t)$. Then, the system in Equation (44) is stable in a finite time $T \leq (1/\alpha(1-\gamma)) \ln\left(\left(\alpha V^{1-\gamma}(x_0) + \beta\right)/\beta\right)$.*

Lemma 2. [34] *Suppose that there exists a continuous positive function V_t, positive real numbers c and $0 < \alpha < 1$, satisfying $\dot{V}_t \leq -c(V(t))^{\alpha}$. Then, the system in Equation (44) is stable in a finite time $T \leq (1/c(1-\alpha))V(X_0)^{1-\alpha}$.*

Lemma 3. *If the undirected graph is connected. The consensus protocol u_i^{nom} shown in Equation (45) can ensure that the state of multi-missile converges in finite time.*

$$u_i^{nom} = sgn\left(\sum_{i,j=1}^{n} a_{ij}(X_j - X_i)\right)\left|\sum_{i,j=1}^{n} a_{ij}(X_j - X_i)\right|^{\beta_i} \tag{45}$$

where a_{ij} are the elements of the weight coefficient matrix. And β_i is a constant, $0 < \beta_i < 1$.

Lemma 4. [35] *If the undirected graph is connected and $1_N^T X = 0$, then $X^T L X \geq \lambda_2(L) X^T X$, where $\lambda_2(L)$ denotes the second smallest eigenvalue of Laplacian matrix L.*

Lemma 5. [36] *Suppose that there exists a series of $x_1, x_2, \cdots, x_n \geq 0$ and $0 < p \leq 1$. Then, the inequality $\sum_{i=1}^{n} x_i^p \geq \left(\sum_{i=1}^{n} x_i\right)^p$ holds.*

Theorem 1. *Subject to the system in Equation (44), in the existence of $k, \varepsilon > 0$, under the action of the guidance command in Equation (46), multiple missiles can achieve consistent convergence of the cooperative variable t_{fi} in a finite time ($T \leq T_1 + T_2$), thereby ensuring that multiple missiles simultaneously arrive at the target.*

$$a_i = (u_i^{nom} - ks_i - \varepsilon sgn(s_i) - k_c)/k_a \tag{46}$$

where $u_i^{nom} = sgn\left(\sum_{i,j=1}^{n} a_{ij}(t_{fj} - t_{fi})\right)\left|\sum_{i,j=1}^{n} a_{ij}(t_{fj} - t_{fi})\right|^{\beta_i}$, $k_c = 1 - \cos(\eta_i)\left(1 + \sin^2(\eta_i)/10\right) + \sin^2(\eta_i)\cos(\eta_i)/5$, $k_a = -r_i \sin(\eta_i)\cos(\eta_i)/5V_{mi}^2$, $\dot{s}_i = -ks_i - \varepsilon sgn(s_i)$.

https://doi.org/10.1017/aer.2023.38 Published online by Cambridge University Press

Proof.

(1) System transformation

Before proving the theorem, some preparations are made as follows.

The derivative of t_{fi} can be presented as

$$\dot{t}_{fi} = \dot{t}_{goi} + 1 \tag{47}$$

From Ref. [16], in order to remove the small-angle assumption of the η_i, an improved estimation method of t_{goi} is chosen as follows

$$t_{goi} = r_i\left(1 + \sin^2(\eta_i)/10\right)/V_{mi} \tag{48}$$

The derivation of t_{goi} is derived as

$$\dot{t}_{goi} = \dot{r}_i\left(1 + \sin^2(\eta_i)/10\right)/V_{mi} + r_i\sin(\eta_i)\cos(\eta_i)\dot{\eta}_i/5V_{mi} \tag{49}$$

Substituting Equations (1–4) into Equation (49), then we can obtain

$$\begin{aligned}\dot{t}_{goi} = &-\cos(\eta_i)\left(1 + \sin^2(\eta_i)/10\right) + \sin^2(\eta_i)\cos(\eta_i)/5 \\ &- a_i r_i\sin(\eta_i)\cos(\eta_i)/5V_{mi}^2\end{aligned} \tag{50}$$

Substituting Equation (50) into Equation (47) and using shorthand notations, Equation (47) can be rewritten as

$$\dot{t}_{fi} = k_c + k_a a_i \tag{51}$$

where

$$\begin{cases} k_c = 1 - \cos(\eta_i)\left(1 + \sin^2(\eta_i)/10\right) + \sin^2(\eta_i)\cos(\eta_i)/5 \\ k_a = -r_i\sin(\eta_i)\cos(\eta_i)/5V_{mi}^2 \end{cases} \tag{52}$$

(2) Convergence of the sliding surface

In order to achieve time-cooperative guidance for multiple missiles, considering the final impact time constraint, a sliding surface is defined as

$$s_i = t_{fi} - t_{fi}(0) - \int_0^t u_i^{nom} dt \tag{53}$$

Take the derivative of sliding surface s_i as

$$\dot{s}_i = \dot{t}_{fi} - u_i^{nom} \tag{54}$$

Apply the reaching law by choosing

$$\dot{s}_i = -ks_i - \varepsilon sgn(s_i) \tag{55}$$

Take the Lyapunov function V_{1i} as

$$V_{1i} = \frac{1}{2}s_i^2 \tag{56}$$

Taking the derivative of V_{1i} with respect to time t, and substituting Equation (55) into it, we can get

$$\dot{V}_{1i} = s_i\dot{s}_i = s_i(-ks_i - \varepsilon sgn(s_i)) \le -ks_i^2 - \varepsilon\,|s_i| \le 0 \tag{57}$$

Based on Equation (56), the following equation is obtained

$$|s_i| = \sqrt{2V_{1i}} \tag{58}$$

Substituting Equation (58) into Equation (57), we have

$$\dot{V}_{1i} \le -ks_i^2 - \varepsilon|s_i| = -2kV_{1i} - \sqrt{2}\varepsilon V_{1i}^{\frac{1}{2}} \tag{59}$$

https://doi.org/10.1017/aer.2023.38 Published online by Cambridge University Press

According to **Lemma 1**, the sliding surface s_i can converge to zero in a finite time T_1, where

$$T_1 \leq (1/k)\ln\left(\left(2kV_{1i}^{\frac{1}{2}}(x_0)+\sqrt{2}\varepsilon\right)/\sqrt{2}\varepsilon\right) \tag{60}$$

(3) Convergence of finite-time cooperative errors
When $s_i = 0$, from Equation (54), the following equation can be obtained as

$$\dot{t}_{fi} = u_i^{nom} \tag{61}$$

Take the Lyapunov function V_{2i} as

$$V_{2i} = \frac{1}{4}\sum_{i,j=1}^{n} a_{ij}\left(t_{fj}-t_{fi}\right)^2 = \frac{1}{2}T_f^T L T_f \tag{62}$$

where $T_f = \left[t_{f1}, t_{f2}, \cdots, t_{fn}\right]^T$ is the vector consisting of the final impact time of each missile and L is the Laplace matrix. Based on the symmetry L due to the assumption of undirected graph, the partial derivative of V_{2i} with respect to t_{fi} can be presented as

$$\frac{\partial V_{2i}}{\partial t_{fi}} = -\sum_{j=1}^{n} a_{ij}\left(t_{fj}-t_{fi}\right) \tag{63}$$

Taking the derivative of V_{2i} with respect to t, combining it with Equations (63), (61) and **Lemma 5**, the following equation can be obtained as

$$\begin{aligned}
\frac{dV_{2i}}{dt} &= \sum_{i=1}^{n}\frac{\partial V_{2i}}{\partial t_{fi}}\dot{t}_{fi} \\
&= -\sum_{i=1}^{n} a_{ij}\left(t_{fj}-t_{fi}\right)\cdot\left(sgn\left(\sum_{j=1}^{n} a_{ij}\left(t_{fj}-t_{fi}\right)\right)\sum_{j=1}^{n} a_{ij}\left(t_{fj}-t_{fi}\right)\right)^{\beta_i} \\
&= -\sum_{i=1}^{n}\left(\left(\sum_{j=1}^{n} a_{ij}\left(t_{fj}-t_{fi}\right)\right)^2\right)^{\frac{1+\beta_i}{2}} \\
&\leq -\left(\sum_{i=1}^{n}\left(\sum_{j=1}^{n} a_{ij}\left(t_{fj}-t_{fi}\right)\right)^2\right)^{\frac{1+\beta_i}{2}}
\end{aligned} \tag{64}$$

when $V_{2i} \neq 0$, we obtain

$$\frac{\sum_{i=1}^{n}\left(\sum_{j=1}^{n} a_{ij}\left(t_{fj}-t_{fi}\right)\right)^2}{V_{2i}} = \frac{T_f^T L^T L T_f}{\frac{1}{2}T_f^T L T_f} \tag{65}$$

According to **Lemma 4**, Equation (65) can be transformed as

$$\frac{T_f^T L^T L T_f}{\frac{1}{2}T_f^T L T_f} \geq 2\lambda_2(L) \tag{66}$$

https://doi.org/10.1017/aer.2023.38 Published online by Cambridge University Press

Table 1. *The initial conditions of missiles*

Number	Position (m)	Initial Heading Angle (deg)	Speed (m/s)
M1	(1500,4000)	30	300
M2	(0,3000)	30	300
M3	(0,100)	30	300

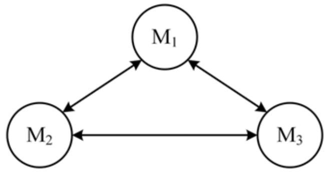

Figure 2. *Communication topology for three missiles.*

Substituting Equation (66) into Equation (64), the following inequality is obtained

$$\frac{dV_{2i}}{dt} \leq -\left(\frac{\sum_{i=1}^{n}\left(\sum_{j=1}^{n} a_{ij}\left(t_{fj}-t_{fi}\right)\right)^2}{V_{2i}} V_{2i}\right)^{\frac{1+\beta_i}{2}}$$

$$\leq -(2\lambda_2(L))^{\frac{1+\beta_i}{2}} V_{2i}^{\frac{1+\beta_i}{2}} \quad (67)$$

According to **Lemma 2**, the final impact time of the missiles can converge to zero in a finite time T_2, where

$$T_2 \leq \left(\frac{1}{\lambda_2(L)^{\frac{1+\beta_i}{2}}(1-\beta_i)}\right) V_{2i}^{\frac{1-\beta_i}{2}}(x_0) \quad (68)$$

□

Remark 2. The sliding surface can converge to zero within a finite T_1, $\lim_{t\to T_1} |s_i| = 0$, which guarantees the establishment of the system in Equation (44). Then, the difference of final impact times can converge to zero in a finite $T \leq T_1 + T_2$, $\lim_{t\to T} \left|t_{fi} - t_{fj}\right| = 0$, which implies multiple missiles can complete a cooperative attack. Since Equation (43), $\lim_{t\to T} \left|t_{goi} - t_{goj}\right| = 0$ also holds.

4.0 Simulation

In this section, simulations were conducted to demonstrate the effectiveness and advantages of the finite-time TSCGL in Equation (48). In all simulations, the initial position of target is located at $(20km, 0km)$. The initial conditions of missiles are shown in Table 1. The communication topology of multiple missiles is given in Fig. 2. The consistency parameter in Equation (45) is selected with $\beta_i = 0.86$. The parameters in sliding mode convergence law shown in Equation (55) are chosen as $k = 0.1$, $\varepsilon = 0.001$. The limitation of guidance command is $a_{\max} = 50m/s^2$. To mitigate the chattering caused by the sign function in Equation (55), the following function is adopted as a replacement

$$sgmf(x) = 2\left(\frac{1}{1+e^{-\tau x}} - \frac{1}{2}\right), \tau > 0 \quad (69)$$

where τ is chosen as 20.

https://doi.org/10.1017/aer.2023.38 Published online by Cambridge University Press

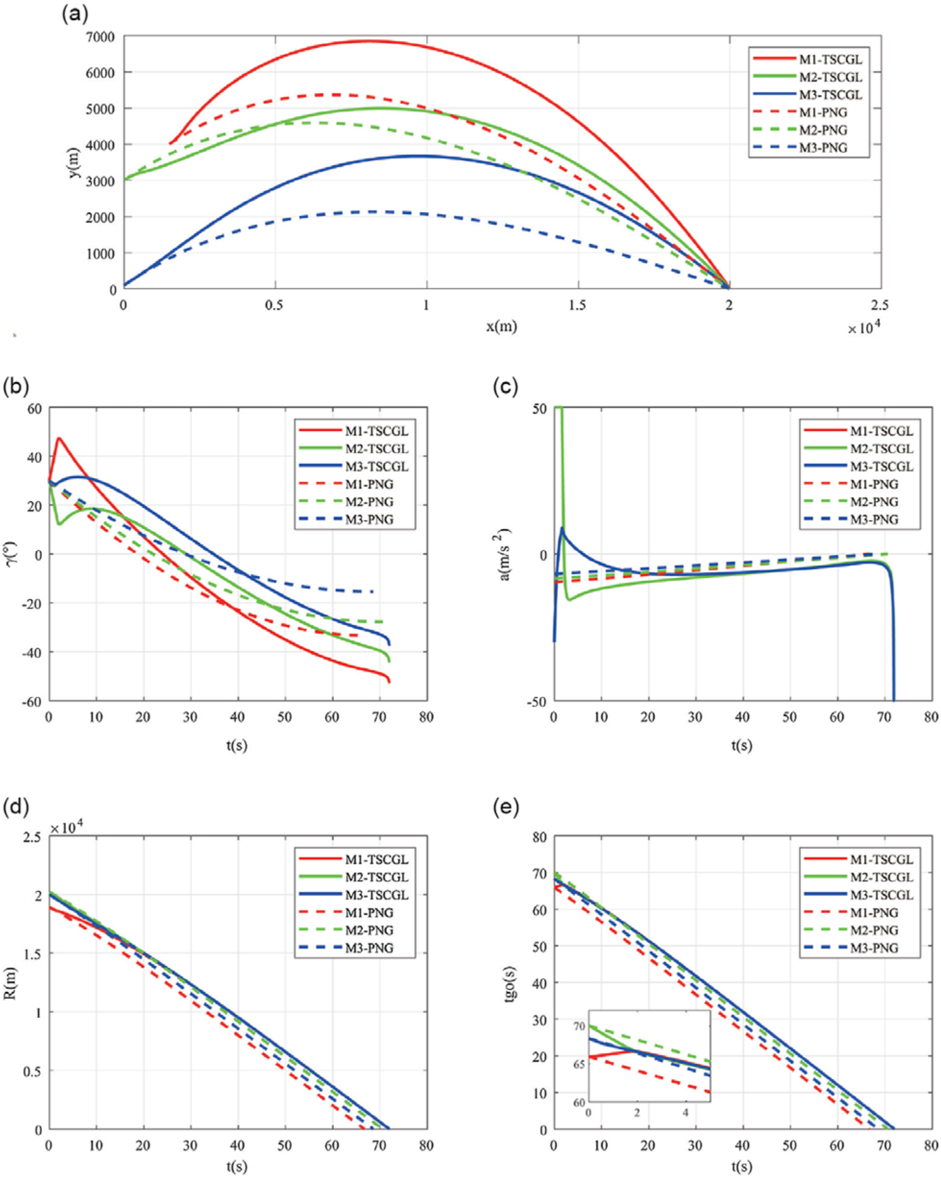

Figure 3. Simulation results of case 1: (a) Trajectory of missiles, (b) Heading angle, (c) Guidance command, (d) Relative distance, (e) Time-to-go.

4.1 Multiple missiles cooperative attack

In this subsection, we compared with PNG algorithm to further demonstrate the superiority of the finite-time TSCGL in Equation (46). The results are presented in Fig. 3, and the attack results are given in Table 2.

From Fig. 3 and Table 2, both the finite-time TSCGL and PNG can attack the target. The miss-distances of the finite-time TSCGL are less than 0.36m. The miss-distances of PNG are at least 1.05m larger than finite-time TSCGL. Compared with PNG, finite-time TSCGL has higher attack accuracy. The trajectories of finite-time TSCGL are more curved than that of PNG. The final heading angle errors

https://doi.org/10.1017/aer.2023.38 Published online by Cambridge University Press

Table 2. Attack results of case 1

	TSCGL			PNG		
Number	M1	M2	M3	M1	M2	M3
Miss-distance (m)	0.2682	0.3551	0.3356	1.9410	3.1914	1.4181
Final heading angle (deg)	−52.91	−44.39	−37.43	−33.30	−27.80	−15.43

between the finite-time TSCGL and PNG are bigger than at least 16.59deg, which implies that finite-time TSCGL has better damage performance. At the beginning of the guidance process, a larger guidance command is required to adjust the posture of the missiles to be consistent. The time-to-go of the finite-time TSCGL can converge within a short time. Compared with PNG, the finite-time TSCGL has faster convergence speed. The final impact time of finite-time TSCGL are 72s with their errors less than 0.1s. The final impact time of PNG are 66.68s, 70.58s, 68.58s and their differences are approximately 4s. In conclusion, the finite-time TSCGL can achieve cooperative attack with higher attack accuracy, better damage performance and faster convergence speed.

4.2 Compared with other methods of estimating time-to-go

In this subsection, another method of estimating t_{go} in Ref. [31] is provided to compare that in Equation (48), which is expressed as

$$t_{goi} = r_i\left(1 + \eta_i^2/10\right)/V_{mi} \tag{70}$$

The results are illustrated in Fig. 4, and the miss-distance are given in Table 3. As can be seen in Fig. 4, multiple missiles can attack the target cooperatively. A striking difference was noted when the method of estimating t_{go} was considered individually in Equation (48) and Equation (70). From Table 3, the miss-distances of Equation (48) are less than 0.36m. The miss-distances of Equation (70) are at least 1.95m larger than Equation (48). By comparison, Equation (48) demonstrates the superiority in attack accuracy. The time-to-go of the two methods can converge within a short time, which indicates that the proposed finite-time TSCGL has fast convergence speed. Similarly, their final impact time are approximately the same, which shows that the proposed finite-time TSCGL can achieve simultaneous attack. Consequently, the different methods of estimating time-to-go mainly affect the attack accuracy rather than the convergence speed and final impact time, further indicating that the proposed finite-time TSCGL has good expandability.

4.3 Cooperative attack with Monte Carlo simulations

In order to further verify the robustness of the finite-time TSCGL in Equation (46), 300 Monte Carlo simulations were performed with different conditions, and the bias are listed in Table 4. The initial conditions of the missiles and the target are the same as in Table 1. The simulation results are illustrated in Figs 5 and 6.

It can be seen from Fig. 5 that multiple missiles can cooperatively attack the target in all Monte Carlo bias scenarios. The distributions of miss distance in Fig. 6 are less than 1.83m. In Table 5, the average mean and standard deviation of the miss-distances are 0.87m, 0.39m. The maximum and minimum are 1.80m, 0.11m. All the statistics can meet the accuracy requirement. Consequently, finite-time TSCGL has strong robustness.

4.4 Expansion to a target with constant speed

Inspired by the concept of predicted interception point (PIP) in Ref. [16], a target with a constant speed is considered to verify the generality of the proposed finite-time TSCGL. The position of virtual stationary

https://doi.org/10.1017/aer.2023.38 Published online by Cambridge University Press

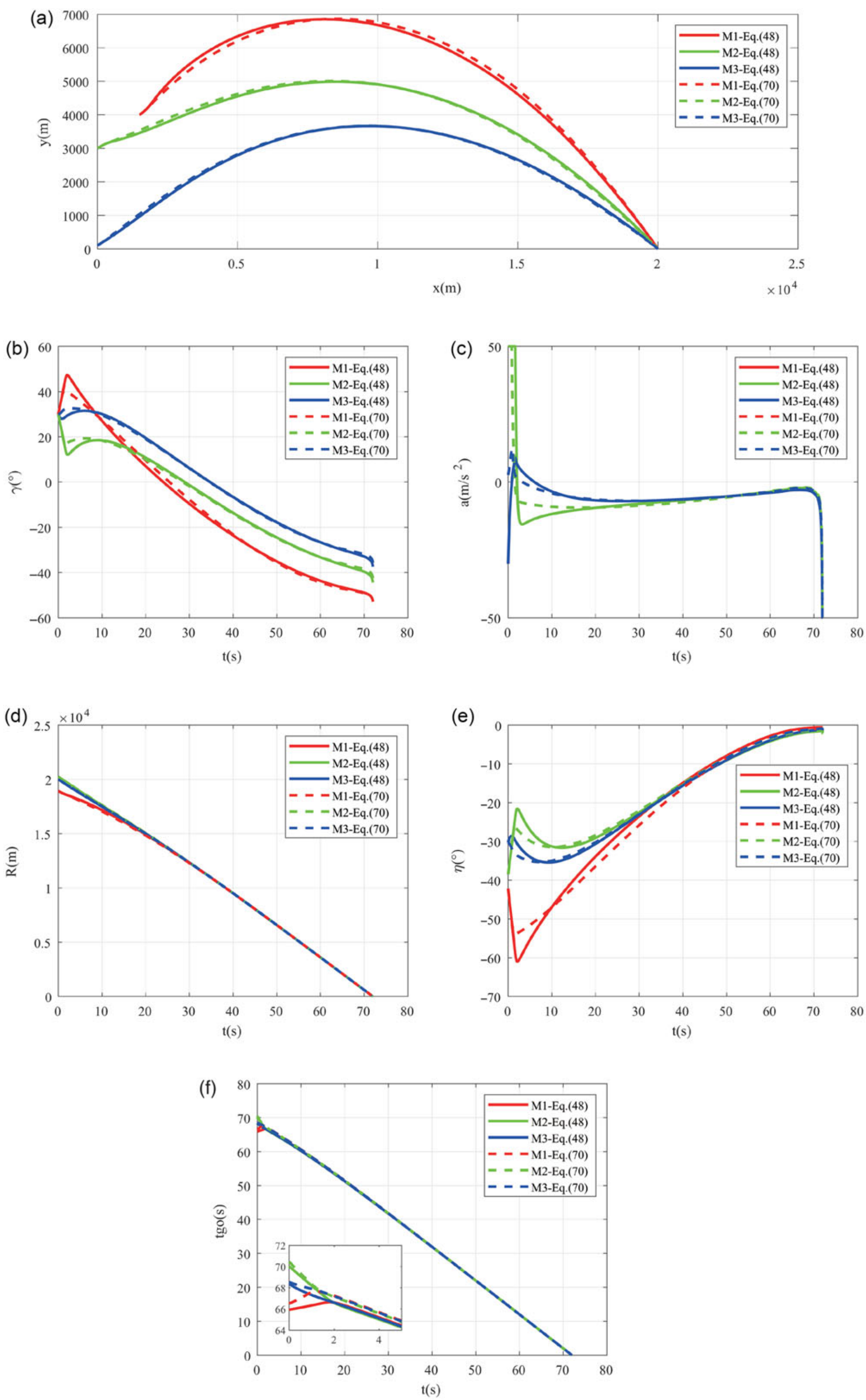

Figure 4. *Simulation results of case 2: (a) Trajectory of missiles, (b) Heading angle, (c) Guidance command, (d) Relative distance, (e) Leading angle, (f) Time-to-go.*

https://doi.org/10.1017/aer.2023.38 Published online by Cambridge University Press

Table 3. *Miss-distance of case 2*

	Equation (48)			Equation (70)		
Number	M1	M2	M3	M1	M2	M3
Miss-distance (m)	0.2682	0.3551	0.3356	2.3338	2.3177	2.3187

Table 4. *Bias of Monte Carlo simulations*

Term		Upper bound	Lower bound
Speed (m/s)		+5	−5
Heading angle (deg)		+3	−3
Position (m)	Direction X	+1000	−1000
	Direction Y	+100	−100

Table 5. *Monte Carlo results of the miss-distance*

Number	Mean (m)	Standard deviation (m)	Maximum (m)	Minimum (m)
M1	0.8462	0.3859	1.8058	0.0831
M2	0.8883	0.3874	1.8268	0.1451
M3	0.8627	0.3912	1.7491	0.0886

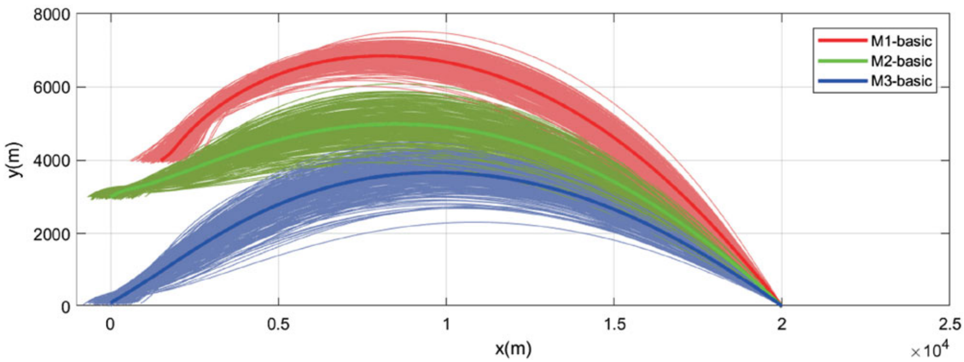

Figure 5. *Trajectory of missiles.*

target can be expressed as follows:

$$\begin{cases} X_{TP} = X_T + V_T \cos\theta_T t_{go} \\ Y_{TP} = Y_T + V_T \sin\theta_T t_{go} \end{cases} \tag{71}$$

where (X_{TP}, Y_{TP}) is the PIP, (X_T, Y_T) is current position of the target, and θ_T is the heading angle of the target.

The target moves with the heading angle of $0deg$ and speed of $20m/s$. It can be seen from Fig. 7 that finite-time TSCGL can simultaneously attack the target with a constant speed under the PIP theory. The miss-distance are $1.31m$, $1.37m$ and $1.39m$, which implies that finite-time TSCGL has high attack accuracy. The time-to-go can converge within a short time, which shows that finite-time TSCGL has fast convergence speed. Therefore, the finite-time TSCGL demonstrates good expandability.

https://doi.org/10.1017/aer.2023.38 Published online by Cambridge University Press

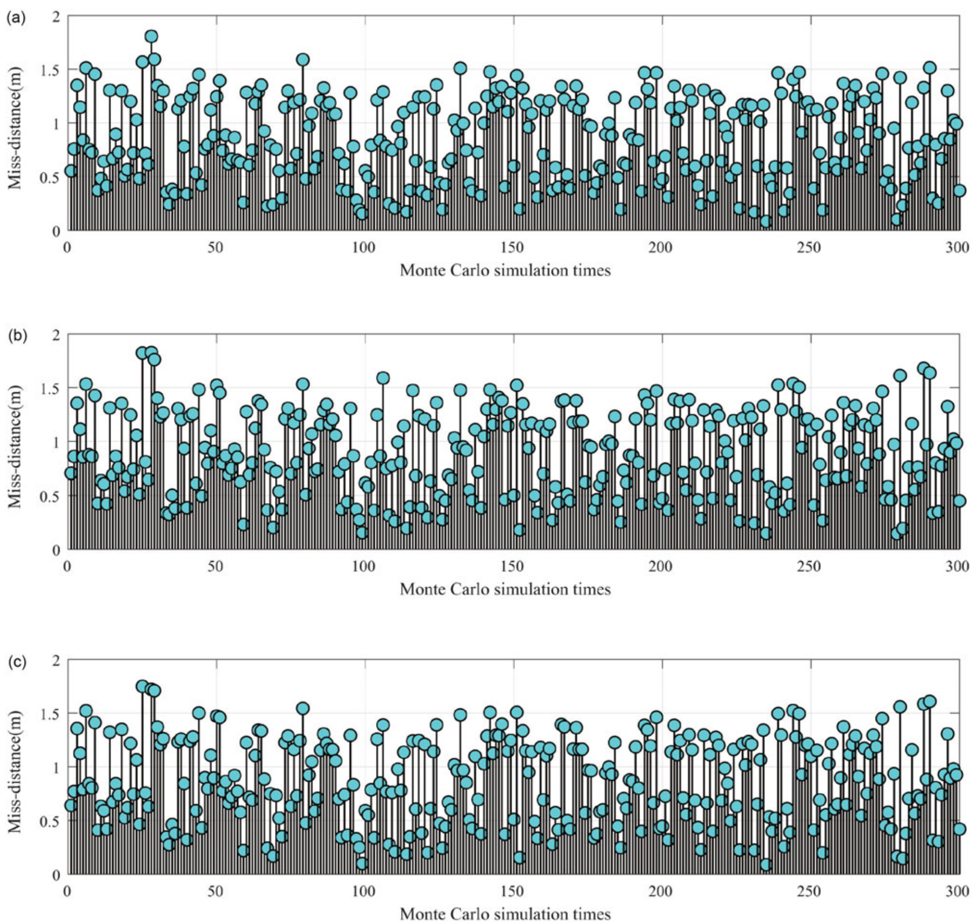

Figure 6. *Miss-distance of case 3: (a) Missile 1, (b) Missile 2, (c) Missile 3.*

5.0 Conclusion

In this paper, we proposed the finite-time TSCGL law, which can ensure that multiple missiles cooperative attack with better damage and convergence performance. The main contributions can be drawn as:

(1) The proposed finite-time TSCGL performs higher attack accuracy and better convergence performance. It can cooperatively attack the target, wherein the miss-distances, convergence time and final errors of impact time are less than $0.36m$, $3s$ and $0.1s$, separately. Compared to traditional PNG, the proposed finite-time TSCGL holds better damage performance with obviously higher final heading angles.

(2) The Monte Carlo simulations show that the proposed finite-time TSCGL has strong robustness. It can achieve simultaneous attack with fast convergence speed. The average mean and standard deviation of the miss-distances are $0.87m$ and $0.39m$, respectively.

(3) The finite-time TSCGL has good expandability. The estimation methods of time-to-go can be replaced, and the proposed method in this paper shows better attack accuracy. Through the PIP theory, it can be expanded against a target with a constant speed.

In the future, the guidance law will be promoted to the three-dimensional space and the complex manoeuver of targets.

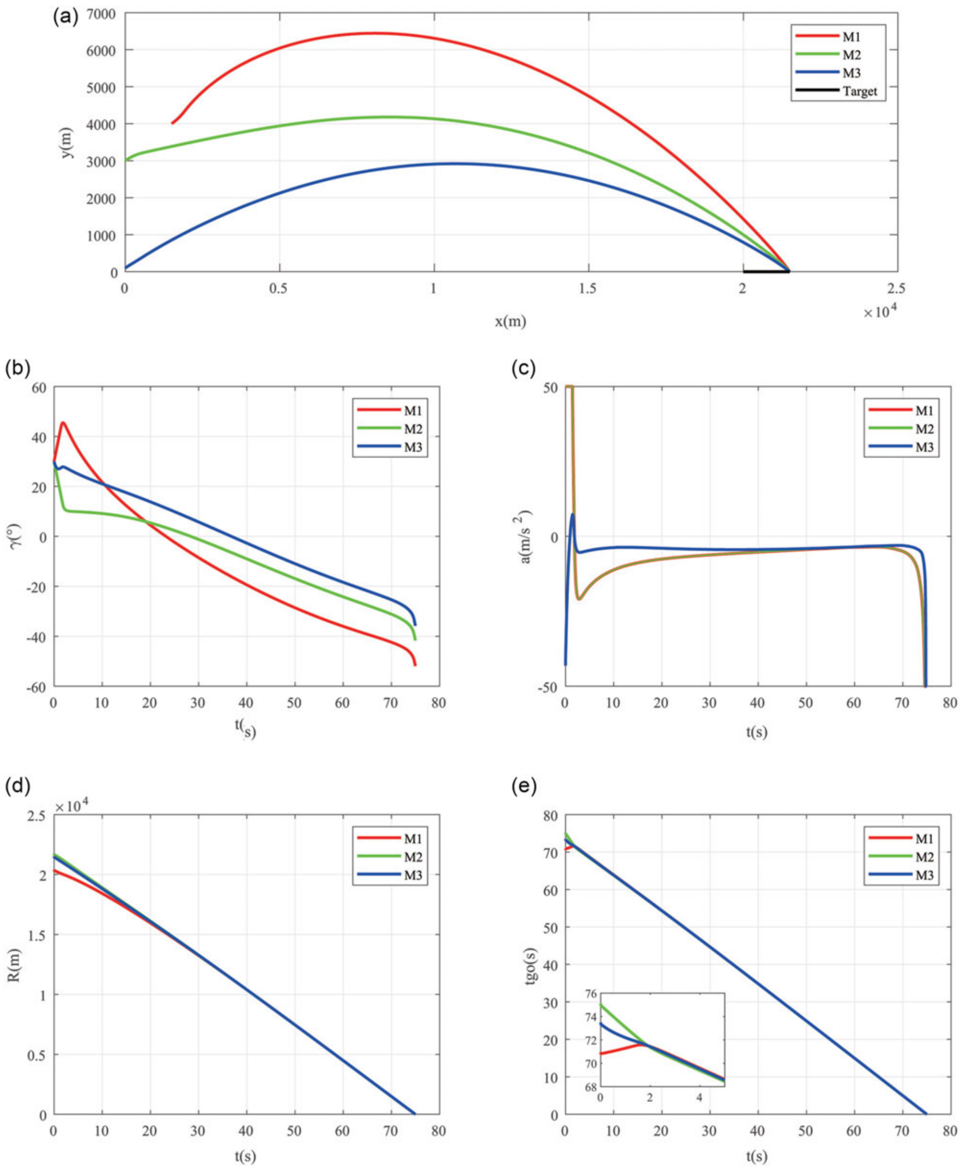

Figure 7. *Simulation results of case 4: (a) Trajectory of missiles, (b) Heading angle, (c) Guidance command, (d) Relative distance, (e) Time-to-go.*

Availability of data and software. The data used to support the findings of this study are included within the article.

Competing interests. The authors declared that they have no conflicts of interest to this work.

Acknowledgements. The authors would like to thank the associate editor and reviewers for their valuable comments and constructive suggestions that helped to improve the paper and presentation significantly.

References

[1] Ryoo C.K., Cho H.J. and Tahk M.J. Optimal guidance laws with terminal impact angle constraint. *J. Guid. Control Dyn.*, 2005, **28**, (4), pp 724–732.

[2] Lee C.H., Jeon I.S. and Lee J.I. Generalized formulation of weighted optimal guidance laws with impact angle constraint. *IEEE Trans. Aerosp. Electron. Syst.*, 2013, **49**, (2), pp 1317–1322.

https://doi.org/10.1017/aer.2023.38 Published online by Cambridge University Press

[3] Lee J.I., Jeon I.S. and Lee C.H. Command-shaping guidance law based on a Gaussian weighting function. *IEEE Trans. Aerosp. Electron. Syst.*, 2014, **50**, (1), pp 772–777.
[4] Ryu M.Y., Lee C.H. and Tahk M.J. New trajectory shaping guidance laws for anti-tank guided missile. *Proc. Inst. Mech. Eng. Part G-J. Aerosp. Eng.*, 2015, **229**, (7), pp 1360–1368.
[5] Zhang Y., Wang X. and Wu H. A distributed cooperative guidance law for salvo attack of multiple anti-ship missiles. *Chinese J. Aeronaut.*, 2015, **28**, (5), pp 1438–1450.
[6] Qin Z., Qi X. and Fu Y. Terminal guidance based on Bézier curve for climb-and-dive maneuvering trajectory with impact angle constraint. *IEEE Access.*, 2018, **7**, pp 2969–2977.
[7] Liu S., Yan B. and Zhang T. Coverage-based cooperative guidance law for intercepting hypersonic vehicles with overload constraint. *Aerosp. Sci. Technol.*, 2022, **126**, p 107651.
[8] Liu S., Yan B. and Zhang T. Three-dimensional coverage-based cooperative guidance law with overload constraints to intercept a hypersonic vehicle. *Aerosp. Sci. Technol.*, 2022, **130**, p 107908.
[9] Jeon I.S., Lee J.I. and Tahk M.J. Impact-time-control guidance law for anti-ship missiles. *IEEE Trans. Control Syst. Technol.*, 2006, **14**, (2) pp 260–266.
[10] Harl N. and Balakrishnan S.N. Impact time and angle guidance with sliding mode control. *IEEE Trans. Control Syst. Technol.*, 2012, **20**, (6) pp 1436–1449.
[11] Chen X. and Wang J. Sliding-mode guidance for simultaneous control of impact time and angle. *J. Guid. Control Dyn.*, 2019, **42**, (2), pp 394–401.
[12] Zhang Y., Wang X. and Ma G. Impact time control guidance law with large impact angle constraint. *Proc. Inst. Mech. Eng. Part G-J. Aerosp. Eng.*, 2015, **229**, (11), pp 2119–2131.
[13] Kim T.H., Park B.G. and Tahk M.J. Bias-shaping method for biased proportional navigation with terminal-angle constraint. *J. Guid. Control Dyn.*, 2013, **36**, (6), pp 1810–1816.
[14] Whang I.H. and Ra W.S. Time-to-go estimation filter for anti-ship missile application. In *2008 SICE Annual Conference*: IEEE, Chofu, Japan, 2008, pp 247–250.
[15] Kim T.H., Park B.G. and Tahk M.J. Time-to-go estimation using guidance command history. *IFAC Proc. Vol.*, 2011, **44**, (1), pp 5531–5536.
[16] Liu S., Yan B. and Zhang T. Guidance law with desired impact time and FOV constrained for antiship missiles based on equivalent sliding mode control. *Int. J. Aerosp. Eng.*, 2021, **2021**, p 15.
[17] Chen X. and Wang J. Optimal control based guidance law to control both impact time and impact angle. *Aerosp. Sci. Technol.*, 2019, **84**, pp 454–463.
[18] Liu J. and Yang J. An event-triggered optimal cooperative guidance law for simultaneous attacks with impact angle constraints. *Aerosp. Sci. Technol.*, 2022, **43**, (5), pp 1343–1357.
[19] Erer K.S. and Tekin R. Impact time and angle control based on constrained optimal solutions. *J. Guid. Control Dyn.*, 2016, **39**, (10), pp 2445–U2451.
[20] Liu S., Yan B. and Huang W. Current status and prospects of terminal guidance laws for intercepting hypersonic vehicles in near space: a review. *J. Zhejiang Univ.-Sci. A (Appl. Phys. Eng.)*, **2023**. doi: 10.1631/jzus.A2200423
[21] An K., Guo Z. and Huang W. A cooperative guidance approach based on the finite-time control theory for hypersonic vehicles. *Int. J. Aeronaut. Space Sci.*, 2022, **23**, pp 169–179.
[22] Zhang S., Guo Y. and Liu Z. Finite-time cooperative guidance strategy for impact angle and time control. *IEEE Trans. Aerosp. Electron. Syst.*, 2021, **57**, (2), pp 806–819.
[23] Liu S., Wang Y. and Li Y. Cooperative guidance for active defence based on line-of-sight constraint under a low-speed ratio. *Aeronaut. J.*, 2022, **2022**, pp 1–19.
[24] Sinha A. and Kumar B. Supertwisting control-based cooperative salvo guidance using leader–follower approach. *IEEE Trans. Aerosp. Electron. Syst.*, 2020, **56**, (5), pp 3556–3565.
[25] Liu S., Yan B. and Zhang T. Three-dimensional cooperative guidance law for intercepting hypersonic targets. *Aerosp. Sci. Technol.*, 2022, **129**, p 107815.
[26] Li B., Lin D. and Wang H. Finite time convergence cooperative guidance law based on graph theory. *Optik*, 2016, **127**, (21), pp 10180–10188.
[27] Liu S., Yan B. and Liu R. Cooperative guidance law for intercepting a hypersonic target with impact angle constraint. *Aeronaut. J.*, 2022, **126**, (1300), pp 1026–1044.
[28] Kumar S.R. and Mukherjee D. Cooperative salvo guidance using finite-time consensus over directed cycles, *IEEE Trans. Aerosp. Electron. Syst.*, 2020, **56**, (2), pp 1504–1514.
[29] Song J., Song S. and Xu S. Three-dimensional cooperative guidance law for multiple missiles with finite-time convergence. *Aerosp. Sci. Technol.*, 2017, **67**, pp 193–205.
[30] Shin H.S., Tsourdos A. and Li K.B. A new three-dimensional sliding mode guidance law variation with finite time convergence, *IEEE Trans. Aerosp. Electron. Syst.*, 2017, **53**, (5), pp 193–205.
[31] Jeon I.S., Lee J.I. and Tahk M.J. Homing guidance law for cooperative attack of multiple missiles. *J. Guid. Control Dyn.*, 2010, **33**, (1), pp 275–280.
[32] Yang G., Fang Y. and Fu W. Cooperative trajectory shaping guidance law for multiple missiles. In *2022 International Conference on Guidance, Navigation and Control (ICGNC)*: IEEE, Harbin, China, 2022, pp 4724–4735.
[33] Yu S. and Yu X. and Shirinzadeh B. Continuous finite-time control for robotic manipulators with terminal sliding mode. *Automatica*, 2005, **41**, (11), pp 1957–1964.

[34] Huang X., Lin W. and Yang B. Global finite-time stabilization of a class of uncertain nonlinear systems. *Automatica*, 2005, **41**, (5), pp 881–888.
[35] Wang Y., Song Y. and Hill D.J. Prescribed-time consensus and containment control of networked multiagent systems. *IEEE T. Cybern.*, 2018, **49**, (4), pp 1138–1147.
[36] Cheng L., Hou Z. and Tan M. Necessary and sufficient conditions for consensus of double-integrator multi-agent systems with measurement noises. *IEEE Trans. Autom. Control.*, 2011, **56**, (8), pp 1958–1963.

Cite this article: Yang G., Fang Y., Ma W., Zhu S. and Fu W. (2024). Cooperative trajectory shaping guidance law for multiple anti-ship missiles. *The Aeronautical Journal*, **128**, 73–91. https://doi.org/10.1017/aer.2023.38